Published in final edited form as:
*Am J Ophthalmol*. 2009 August ; 148(2): 242–248.e1. doi:10.1016/j.ajo.2009.03.004.

# Comparison of Clinically-Relevant Findings from High Speed Fourier Domain and Conventional Time Domain Optical Coherence Tomography

**Pearse A. Keane**[1], **Rizwan A. Bhatti**[1], **Jacob W. Brubaker**[2], **Sandra Liakopoulos**[3], **Srinivas R. Sadda**[1], and **Alexander C. Walsh**[1]

[1]Doheny Image Reading Center, Doheny Eye Institute, Keck School of Medicine of the University of Southern California, Los Angeles, California

[2]University of Utah, Utah

[3]Department of Vitreoretinal Surgery, Center for Ophthalmology, University of Cologne, Germany

## Abstract

**Purpose—**To compare the sensitivities of high speed Fourier domain optical coherence tomography (FDOCT) and conventional time domain (TD)-OCT for the detection of clinical findings important in the management of common vitreoretinal disorders.

**Design—**Prospective observational study.

**Methods—**FDOCT scans (128 B-scans × 512 A-scans) were obtained using a prototype instrument (3D-OCT, Topcon, Japan) in 50 eyes of 28 consecutive patients undergoing conventional high resolution (6 B-scans × 512 A-scans) TDOCT imaging (StratusOCT, Carl Zeiss Meditec, USA). Each image set was reviewed independently for the presence of clinical findings of interest, and device sensitivities calculated.

**Results—**The average sensitivity for detection of all features in this study was 94% for FDOCT and 60% for TDOCT. Clinical findings were identical between devices in 18% (9/50) of cases. FDOCT detected features that were not visible on conventional OCT scans in 78% (39/50) of cases. FDOCT was more sensitive than TDOCT for the detection of multiple findings, including: diffuse intraretinal edema (87% versus 60.9%), subretinal fluid (100% versus 46.2%), large pigment epithelium detachments (100% versus 81%), and subretinal tissue (100% versus 61.5%).

**Conclusions—**FDOCT appears superior to TDOCT for the detection of many clinically relevant features of vitreoretinal disease. The greater sensitivity of FDOCT systems, for the detection of intraretinal and subretinal fluid, may be of particular importance for the treatment of patients with

Correspondence and reprint requests to Alexander C. Walsh, MD, Doheny Eye Institute, 1450 San Pablo Street, Los Angeles, CA 90033, Tel: (323) 632-9777, Fax: (323) 4426460, Email: awalsh@doheny.org.

**Financial Disclosures:** Drs. Walsh and Sadda are co-inventors of Doheny intellectual property related to optical coherence tomography that has been licensed by Topcon Medical Systems, and are members of the scientific advisory board for Heidelberg Engineering.

**Contributions of Authors:** Conception and design (ACW); analysis and interpretation (ACW, SRS); writing the article (PAK); critical revision of the article (RAB, SL); final approval of the article (ACW, SRS); data collection (JWB, SL, ACW); statistical expertise (PAK, ACW); literature search (PAK, RAB).

neovascular AMD. FDOCT is likely to supplant TDOCT as the standard of care for retinal specialists in the near future.

### Keywords

Optical Coherence Tomography; Fourier Domain; Spectral Domain

## Introduction

Optical coherence tomography (OCT), first described by Huang et al. in 1991, allows high-resolution cross-sectional (tomographic) images of the neurosensory retina to be obtained in a non-invasive manner.[1] StratusOCT (Carl Zeiss Meditec, Dublin, CA) has an axial resolution of 8-10 μm and is the most commonly used OCT system worldwide.[2] OCT images are generated by comparing the time delay and intensity of light waves scattered from tissue to those traveling in a known reference path. In time-domain (TD)-OCT systems such as StratusOCT, light waves returning from different retinal structures are assessed by varying the position of a reference mirror. Although TDOCT systems are capable of generating high-resolution images, they are limited by a low scanning speed (400 A-scans per second for StratusOCT) and thus, only sparse coverage of the macular area is possible (Figure 1).[2]

In recent years, the image acquisition speed of OCT systems has increased by many orders of magnitude. In these systems, light waves returning from the eye enter a diffraction grating and the resulting spectral fringe pattern is registered using a charge coupled device camera – a mathematical (Fourier) transformation is then applied to obtain information regarding the time delay and intensity of these waves.[3-6] These "high speed" OCT systems are commonly referred to as spectral domain, or Fourier domain (FD)-OCT. Since the light waves returning from different axial depths are measured simultaneously, without the need for a mobile reference mirror, each A-scan can be acquired 50-100 times more quickly than in TDOCT systems. The high A-scan acquisition speed (typically over 20,000 A-scans per second) of FDOCT allows more complete coverage of the macular area via dense raster scanning (Figure 1).[4, 6] In addition to these speed advantages, recently released, commercially available, FDOCT systems have incorporated improved superluminescent diode light sources, allowing incremental improvements in axial image resolution.[7]

On its initial introduction, OCT was used predominantly for the qualitative evaluation of disorders of the vitreoretinal interface (e.g. macular holes) and for the quantitative assessment of retinal thickening (e.g. diabetic macular edema).[8] Clinical usage has since been extended to macular disorders with more complex morphological features (e.g. neovascular age-related macular degeneration (AMD)).[9, 10] The improvements offered by FDOCT technology may facilitate improved understanding of, and treatment for, these disorders, as well as extending the range of OCT applications to include the assessment of inherited retinal degenerations and non-exudative ("dry") AMD.[11-13]

In this study, we compare the sensitivities of a FDOCT system (3D-OCT 1000, Topcon, Japan) and a TDOCT system (StratusOCT), for the detection of tomographic features relevant to the diagnosis and management of common vitreoretinal disorders.

## Materials and Methods

### Data Collection

For this prospective study, FDOCT images were obtained from consecutive patients undergoing conventional TDOCT imaging between September 15th and October 3rd 2006 at the Doheny Eye Institute. Approval for data collection and analysis was obtained from the

institutional review board of the University of Southern California. The research adhered to the tenets set forth in the Declaration of Helsinki.

TDOCT scans were obtained using the Radial Lines protocol of 6 high-resolution B-scans on a single StratusOCT machine (6 B-scans × 512 A-scans, StratusOCT, Carl Zeiss Meditec, Dublin, CA). This system acquires 400 A-scans per second with an axial resolution of 8-10 μm. In the StratusOCT Radial Lines protocol, each of the 6 radial line scans covers 6 mm and a complete set can be acquired in approximately 8-10 seconds.[2]

FDOCT images were obtained using a raster scan protocol on a prototype instrument (128 B-scans × 512 A-scans, 3D-OCT, Topcon, Japan). This system acquires 18,000 A-scans per second with an axial resolution of 6 μm. Using the 3D-OCT raster scan protocol, the complete dataset is acquired in fewer than 3.7 seconds.[14] For both devices, image sets centered on the fovea were obtained. No patients were excluded from the study on the basis of media opacity or ocular pathology.

### Grading of Tomographic Features

Each set of OCT scans was reviewed independently by retinal specialists certified in OCT grading by the Doheny Image Reading Center (ACW, SRS), using a standard protocol to identify commonly graded OCT features (Table 1). After this review, a standard form was completed by each grader for each image set: each tomographic feature was recorded as “Visible”, “Questionable”, “Not Visible”, or “Cannot Grade”. Disagreement regarding the detection of features was resolved by open adjudication.

### Assessment of External Limiting Membrane

For each FDOCT dataset, the horizontal OCT B-scan passing closest to the point of fixation was identified and exported to Adobe Photoshop (version 7.0, Adobe Inc). The horizontal radial line scan was also chosen from each TDOCT dataset, and exported to Adobe Photoshop in a similar fashion. A line identifying the external limiting membrane was traced, where visible, on a separate layer using the pencil tool (Figure 2). Drawn pixels were then counted using the histogram function. Subsequently, these data were converted to percentages by dividing the number of painted pixels by the image width.

### Statistical Methods

The ground truth for each case was determined by merging the findings from both methods to generate the maximal possible level of detection for each finding. The sensitivity of each imaging method, for the detection of each tomographic feature, was then calculated as the proportion of true positives correctly identified as such (Sensitivity = True positives/(True positives + False negatives)). 95% confidence intervals for the sensitivity of each method were also determined.

For each OCT device, the percentage ELM visibility was compared using a Wilcoxon signed-rank test. $P < 0.05$ was considered to be statistically significant. Statistical analysis and was performed using commercially available software (Intercooled Stata for Windows, Version 9, Statacorp LP, USA).

## Results

### Tomographic Features

The average sensitivity for detection of all features in the study was 94% for FDOCT and 60% for TDOCT. If questionable grades were excluded, the overall sensitivity for FDOCT decreased to 92%, and for TDOCT to 59%. Tomographic features were identical between devices in 18%

(9/50) of cases. FDOCT detected features that were not visible on conventional TDOCT scans in 78% (39/50) of cases. In 6 cases (12%), tomographic features, visible on TDOCT, were not evident on FDOCT.

The detection sensitivity for features of the preretinal space and macular holes is shown in Table 1. When questionable grades were included, FDOCT was more sensitive than TDOCT for the detection of the posterior hyaloid face (100% versus 73.3%), vitreomacular traction (100% versus 42.9%), epiretinal membrane (95.5% versus 63.6%), and lamellar holes (60% versus 40%).

The detection sensitivity for retinal, subretinal, and retinal pigment epithelium (RPE) findings is shown in Table 2. When questionable grades were included, FDOCT was more sensitive than TDOCT for the detection of multiple findings, including: diffuse intraretinal edema (87% versus 60.9%), subretinal fluid (100% versus 46.2%), large pigment epithelium detachments (100% versus 81%), and subretinal tissue (100% versus 61.5%). Visualization of photoreceptor outer segment disruption was also facilitated by FDOCT (94.4% versus 33.3%).

### External Limiting Membrane

On average, the ELM was visible across 39% of the TDOCT B-scans in this cohort (range 3-76%). The ELM was visible across an average of 56% of the FDOCT scans (range 5-95%). The difference between these two populations was statistically significant ($p<0.00001$) and represented an increase in the extent of visualization of 45%.

## Discussion

In this prospective cross-sectional study, we provide preliminary evidence of the increased sensitivity of FDOCT for the detection of retinal features of importance in the diagnosis and management of macular disease.

FDOCT was more sensitive than TDOCT for detection of the structural features of the vitreomacular interface (e.g. posterior hyaloid face, vitreomacular traction, epiretinal membrane) (Figure 3). In the most commonly used TDOCT scanning protocols, radial line scans are positioned to intersect on the foveal center point to minimize the chance that critical macular findings will be missed in patients with significant pathology or poor fixation. Even in cases of accurate scanning, TDOCT may fail to detect focal abnormalities occurring in a juxta- or extra-foveal position if they fall between the radial scan lines. The increased coverage of the macular area afforded by FDOCT is also useful for the evaluation of cases where vitreomacular interface abnormalities occur over a broad area. FDOCT also allows improved detection of epiretinal membranes both because of dense coverage and because of higher resolution light sources that have improved the axial resolution of modern OCT instruments. This finding, and the improved visualization of the posterior hyaloid face, may shed additional light onto the pathogenesis of these disorders.[15, 16] Moreover, volumetric rendering of FDOCT datasets may allow improved qualitative evaluation of the tractional forces occurring in these disorders and serve as a guide for surgical decision-making.[17] Although the sample size in this study is too small to draw firm conclusions, it appears that the perifoveal concentration of TDOCT radial line scans is often adequate for the initial diagnosis of full-thickness macular holes. However, other studies have suggested that the increased axial resolution of FDOCT may provide additional prognostic information for patients with this disorder and aid the assessment of postoperative anatomic outcomes.[14, 18, 19]

In this study, FDOCT was more sensitive than TDOCT for the detection of intraretinal fluid accumulation in the form of diffuse sponge-like retinal edema. Subretinal fluid accumulation was also more commonly identified using FDOCT. Detection of these features plays a critical

role in the treatment of both retinal and choroidal vascular disorders. In the PrONTO study, treatment of neovascular AMD with ranibizumab was based, in part, on OCT criteria: a loss of five letters of visual acuity in conjunction with intra- or subretinal fluid on OCT being an indication for retreatment.[9] In addition, retreatment in the CATT (**C**omparison of **A**ge-Related Macular Degeneration **T**reatments **T**rials) and IVAN (**I**nhibit **V**EGF in **A**ge-related choroidal **N**eovascularization) trials, comparing the safety and efficacy of ranibizumab with that of bevacizumab, is determined primarily by the presence of intraretinal, subretinal, or sub-RPE fluid on OCT. Areas of hyperreflective tissue in the subretinal space (corresponding to fibrovascular tissue, hemorrhage, lipid or thick fibrin), termed “subretinal tissue”, were also more readily detected on FDOCT. In disorders such as neovascular AMD, the presence of these areas on OCT may be an indicator of reduced visual acuity.[20]

Evidence from this report also suggests that the increased axial resolution and sensitivity of FDOCT allows better detection of fine structures such as the external limiting membrane (ELM) and of photoreceptor outer segment disruption, when present. Disruption of the ELM-photoreceptor complex plays a critical role in the accumulation of lipoproteinaceous fluid in the neurosensory retina.[21] Detection of an intact ELM on OCT may be an important prognostic indicator in retinal vascular diseases such as central retinal vein occlusion.[22] Evaluation of the photoreceptor outer segments is of particular importance in patients with retinal dystrophies and those presenting with unexplained visual loss. In many cases, photoreceptor outer segment disruption is correlated with reductions in visual acuity[23, 24] – the improved capability of FDOCT for photoreceptor outer segment visualization may allow better monitoring of disease progression in patients with these disorders.[13]

Finally, FDOCT appears superior to TDOCT for the evaluation of the RPE and inner choroid. Large pigment epithelium detachments were less frequently detected on TDOCT than on FDOCT. Choroidal vascular disorders, such as neovascular AMD, are commonly associated with serous, hemorrhagic, or fibrovascular PEDs.[25] Accurate delineation of these features is critical for both qualitative and quantitative evaluation of these disorders. In this report, FDOCT was also more sensitive for the detection of small PEDs corresponding to drusen. Due to their slower acquisition speed, TDOCT images are more prone to motion artifacts, making the identification of drusen more difficult.[12] The advent of FDOCT, combined with advances in image analysis software may extend the clinical utility of OCT to include the evaluation of drusen, thus providing additional information on the natural history, and effects of intervention on, patients with AMD.

The increased sensitivity of FDOCT over TDOCT, detected in this study, is predominantly attributable to the increased sampling of the macular area facilitated by high-speed image acquisition in these systems. However, in 12% of cases, TDOCT was capable of identifying tomographic features that were not visible using FDOCT – mainly due to poor image quality in the FDOCT cases. In four of these cases, FDOCT failed to detect the presence of small intraretinal cystoid spaces. In the other two cases, FDOCT failed to detect a lamellar hole and a highly reflective intraretinal interface. In the FDOCT raster scan protocol used in this study (128 B-scans × 512 A-scans over a 6×6 mm area), each B-scan is separated by approximately 45 μm. TDOCT imaging was performed using a radial lines protocol that concentrates image acquisition at the foveal center and is, therefore, sometimes capable of detecting small lesions not captured using a grid scanning protocol. FDOCT scanning protocols are still evolving and the optimal scan density for maximum clinical applicability remains unknown.

One major limitation of this study is the relatively small sample size. In addition, our findings were limited to a single FDOCT system: 3D-OCT 1000 by Topcon. Although it is likely that other FDOCT systems offer similar advantages over TDOCT, further study will be required to confirm this hypothesis and to assess the relative merits of each platform. A further limitation

of our study was our inability to completely mask from the graders the OCT system from which images under evaluation were obtained – we attempted to minimize this potential source of bias through the use of a dual-grader process. Finally, our study was focused on qualitative comparisons of OCT images – not quantitative comparisons of the two technologies. Quantitative measurements obtained from OCT systems now constitute a critical component of many clinical trials for macular disorders.[26] As a result, the accuracy of the automated image analysis software for OCT systems may be at least as important as the hardware specifications for these systems.

In summary, FDOCT appears superior to TDOCT for the detection of many clinically relevant features of vitreoretinal disease. The greater sensitivity of FDOCT systems, for the detection of intraretinal and subretinal fluid, may be of particular importance for the treatment of patients with neovascular AMD. FDOCT is likely to supplant TDOCT as the standard of care for retinal specialists in the near future.

## Acknowledgments

**Institutional Review Board:** Approval for data collection and analysis was obtained from the institutional review board of the University of Southern California.

This study is HIPAA compliant.

**Funding / Support:** Supported in part by NIH Grant EY03040 and NEI Grant R01 EY014375

**Other Acknowledgements:** None

## References

1. Huang D, Swanson EA, Lin CP, Schuman JS, Stinson WG, Chang W, Hee MR, Flotte T, Gregory K, Puliafito CA, et al. Optical coherence tomography. Science 1991;254:1178–81. [PubMed: 1957169]
2. Schuman, JS.; Puliafito, CA.; Fujimoto, JG. Optical Coherence Tomography of Ocular Diseases. Vol. 2nd. Slack Inc.; 2004.
3. Chen TC, Cense B, Pierce MC, Nassif N, Park BH, Yun SH, White BR, Bouma BE, Tearney GJ, de Boer JF. Spectral domain optical coherence tomography: ultra-high speed, ultra-high resolution ophthalmic imaging. Arch Ophthalmol 2005;123:1715–20. [PubMed: 16344444]
4. Schmidt-Erfurth U, Leitgeb RA, Michels S, Povazay B, Sacu S, Hermann B, Ahlers C, Sattmann H, Scholda C, Fercher AF, Drexler W. Three-dimensional ultrahigh-resolution optical coherence tomography of macular diseases. Invest Ophthalmol Vis Sci 2005;46:3393–402. [PubMed: 16123444]
5. Wojtkowski M, Bajraszewski T, Gorczyńska I, Targowski P, Kowalczyk A, Wasilewski W, Radzewicz C. Ophthalmic imaging by spectral optical coherence tomography. Am J Ophthalmol 2004;138:412–9. [PubMed: 15364223]
6. Wojtkowski M, Srinivasan V, Fujimoto JG, Ko T, Schuman JS, Kowalczyk A, Duker JS. Three-dimensional retinal imaging with high-speed ultrahigh-resolution optical coherence tomography. Ophthalmology 2005;112:1734–46. [PubMed: 16140383]
7. Drexler W, Fujimoto JG. State-of-the-art retinal optical coherence tomography. Prog Ret Eye Res 2008;27:45–88.
8. Voo I, Mavrofrides EC, Puliafito CA. Clinical applications of optical coherence tomography for the diagnosis and management of macular diseases. Ophthalmol Clin North Am 2004;17:21–31. [PubMed: 15102511]
9. Fung AE, Lalwani GA, Rosenfeld PJ, Dubovy SR, Michels S, Feuer WJ, Puliafito CA, Davis JL, Flynn HW, Esquiabro M. An optical coherence tomography-guided, variable dosing regimen with intravitreal ranibizumab (Lucentis) for neovascular age-related macular degeneration. Am J Ophthalmol 2007;143:566–83. [PubMed: 17386270]

10. Kaiser PK, Blodi BA, Shapiro H, Acharya NR, MARINA Study Group. Angiographic and Optical Coherence Tomographic Results of the MARINA Study of Ranibizumab in Neovascular Age-Related Macular Degeneration. Ophthalmology 2008;114:1868–75. [PubMed: 17628683]
11. Gorczynska I, Srinivasan V, Vuong LN, Chen RW, Liu JJ, Reichel E, Wojtkowski M, Schuman JS, Duker J, Fujimoto JG. Projection OCT fundus imaging for visualizing outer retinal pathology in non-exudative age related macular degeneration. Br J Ophthalmol. 2008 Jul 28;Epub ahead of print
12. Khanifar AA, Koreishi AF, Izatt JA, Toth CA. Drusen Ultrastructure Imaging with Spectral Domain Optical Coherence Tomography in Age-related Macular Degeneration. Ophthalmology 2008;115:1883–90. [PubMed: 18722666]
13. Lim JI, Tan O, Fawzi AA, Hopkins JJ, Gil-Flamer JH, Huang D. A Pilot Study of Fourier-Domain Optical Coherence Tomography of Retinal Dystrophy Patients. Am J Ophthalmol 2008;146:417–426. [PubMed: 18635153]
14. Hangai M, Ojima Y, Gotoh N, Inoue R, Yasuno Y, Makita S, Yamanari M, Yatagai T, Kita M, Yoshimura N. Three-dimensional imaging of macular holes with high-speed optical coherence tomography. Ophthalmology 2007;114:763–73. [PubMed: 17187861]
15. Legarreta JE, Gregori G, Knighton RW, Punjabi OS, Lalwani GA, Puliafito CA. Three-dimensional spectral-domain optical coherence tomography images of the retina in the presence of epiretinal membranes. Am J Ophthalmol 2008;145:1023–30. [PubMed: 18342830]
16. Michalewski J, Michalewska Z, Cisiecki S, Nawrocki J. Morphologically functional correlations of macular pathology connected with epiretinal membrane formation in spectral optical coherence tomography (SOCT). Graefes Arch Clin Exp Ophthalmol 2007;245:1623–31. [PubMed: 17479277]
17. Koizumi H, Spaide RF, Fisher YL, Freund KB, Klancnik JM, Yannuzzi LA. Three-dimensional evaluation of vitreomacular traction and epiretinal membrane using spectral-domain optical coherence tomography. Am J Ophthalmol 2008;145:509–17. [PubMed: 18191099]
18. Michalewska Z, Michalewski J, Cisiecki S, Adelman R, Nawrocki J. Correlation between foveal structure and visual outcome following macular hole surgery: a spectral optical coherence tomography study. Graefes Arch Clin Exp Ophthalmol 2008;246:823–30. [PubMed: 18386040]
19. Sano M, Shimoda Y, Hashimoto H, Kishi S. Restored Photoreceptor Outer Segment and Visual Recovery After Macular Hole Closure. Am J Ophthalmol 2009;147:313–18. e1. [PubMed: 18835472]
20. Keane PA, Liakopoulos S, Chang KT, Wang M, Dustin L, Walsh AC, Sadda SR. Relationship Between Optical Coherence Tomography Retinal Parameters and Visual Acuity in Neovascular Age-Related Macular Degeneration. Ophthalmology 2008;115:2206–14. [PubMed: 18930551]
21. Marmor MF. Mechanisms of fluid accumulation in retinal edema. Doc Ophthalmol 1999;97:239–49. [PubMed: 10896337]
22. Yamaike N, Tsujikawa A, Ota M, Sakamoto A, Kotera Y, Kita M, Miyamoto K, Yoshimura N, Hangai M. Three-dimensional imaging of cystoid macular edema in retinal vein occlusion. Ophthalmology 2008;115:355–62. e2. [PubMed: 17675242]
23. Ergun E, Hermann B, Wirtitsch M, Unterhuber A, Ko TH, Sattmann H, Scholda C, Fujimoto JG, Stur M, Drexler W. Assessment of central visual function in Stargardt's disease/fundus flavimaculatus with ultrahigh-resolution optical coherence tomography. Invest Ophthalmol Vis Sci 2005;46:310–6. [PubMed: 15623790]
24. Wirtitsch MG, Ergun E, Hermann B, Unterhuber A, Stur M, Scholda C, Sattmann H, Ko TH, Fujimoto JG, Drexler W. Ultrahigh resolution optical coherence tomography in macular dystrophy. Am J Ophthalmol 2005;140:976–83. [PubMed: 16376639]
25. Gass, JD. Stereoscopic Atlas of Macular Diseases: Diagnosis and Treatment. Vol. 4th. Vol. 1. St Louis: CV Mosby; 1997. Chapter 2
26. Diabetic Retinopathy Clinical Research Network. A randomized trial comparing intravitreal triamcinolone acetonide and focal/grid photocoagulation for diabetic macular edema. Ophthalmology 2008;115:1447–9. e1–10. [PubMed: 18662829]

## Abbreviations

**AMD**

| | |
|---|---|
| | age-related macular degeneration |
| **OCT** | optical coherence tomography |
| **PED** | pigment epithelium detachment |
| **RPE** | retinal pigment epithelium |
| **IS-OS** | inner segment-outer segment |
| **FD** | Fourier domain |

## Biography

**Biosketch** Pearse Keane, MRCOphth, currently works as a Clinical Research Fellow in the Doheny Eye Institute, Los Angeles. Dr Keane obtained his medical degree from University College Dublin, Ireland and, prior to his current post, underwent clinical ophthalmology training in Ireland. Dr Keane's primary area of interest is the use of advanced retinal imaging techniques in the study of neovascular age-related macular degeneration.

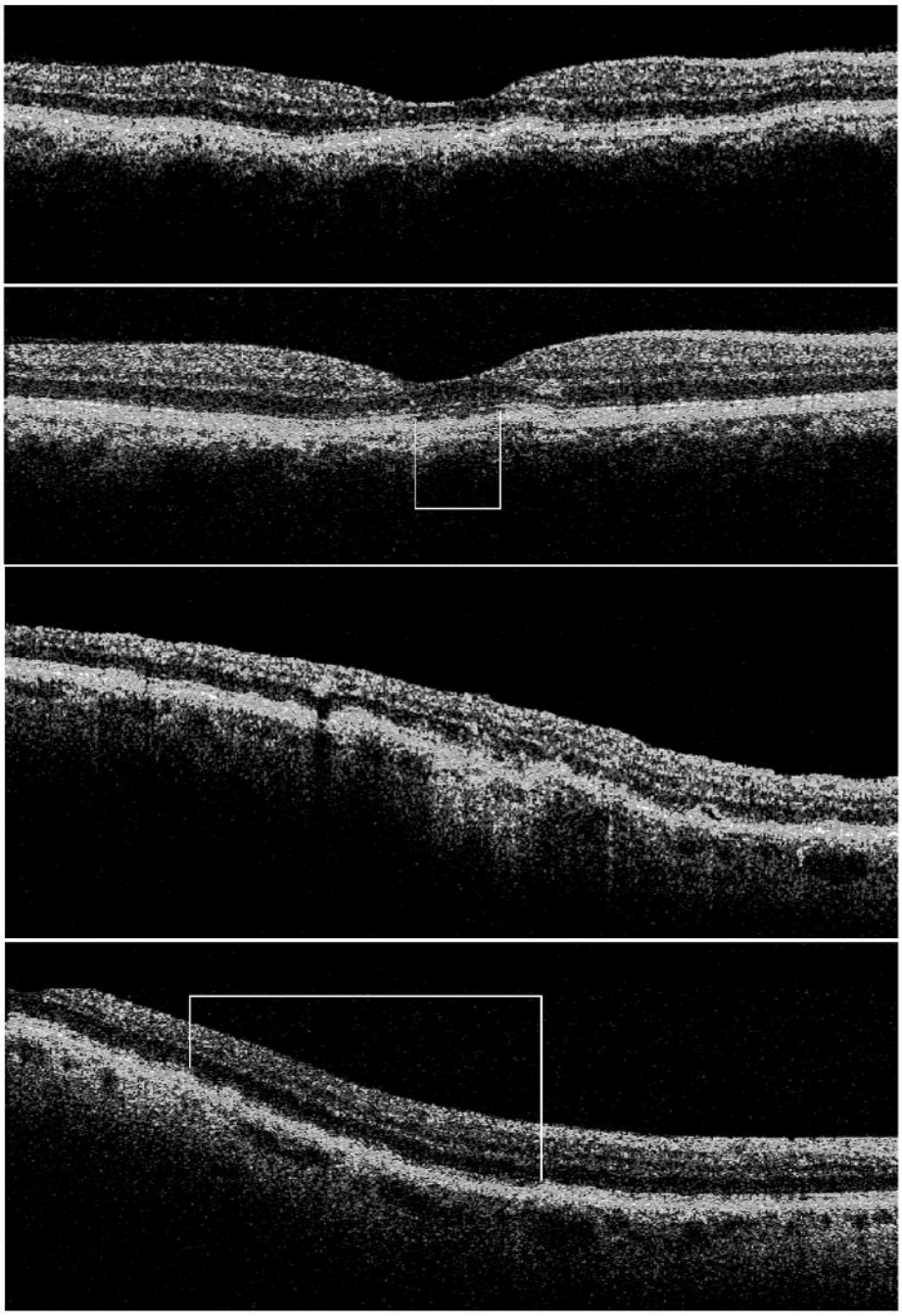

**Figure 1.**
Retinal Coverage with OCT. (Left) Conventional Time domain OCT data showing sparse coverage of radial line B-scans. (Right) Fourier domain OCT data projected onto a fundus image showing dense coverage of the macular area by 3D-OCT B-scans.

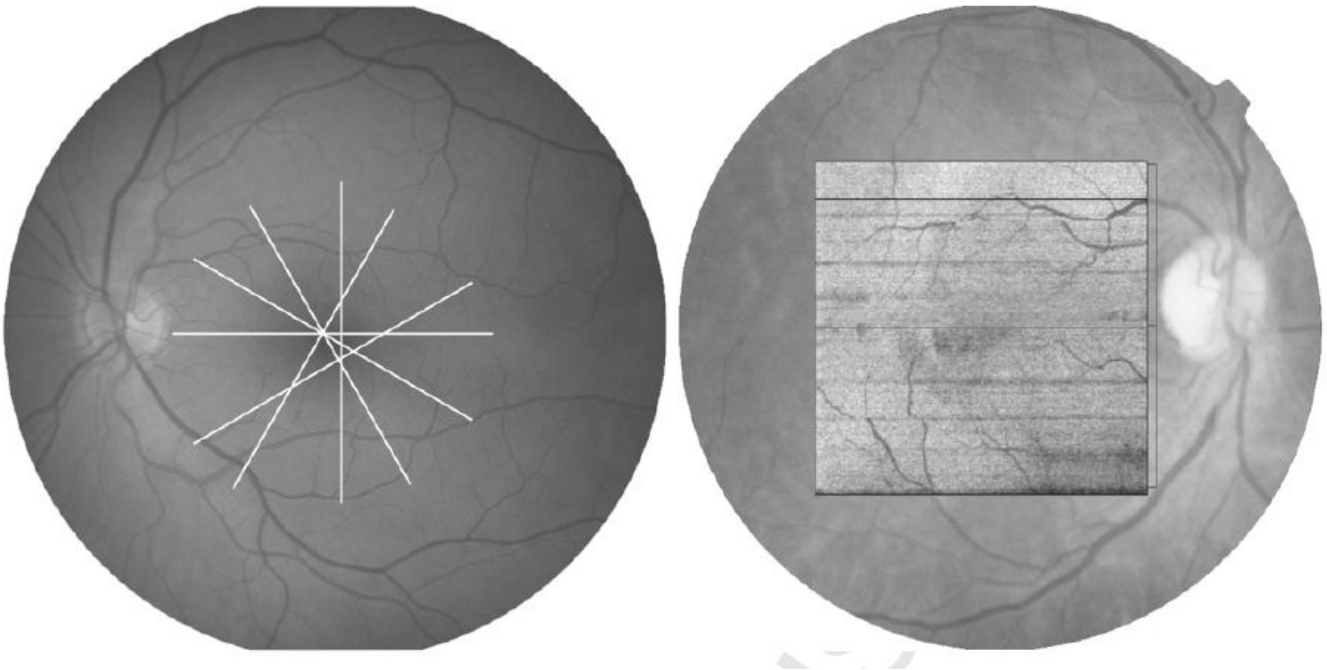

**Figure 2.**
Fourier domain (FD)-OCT (top left) and Time domain (TD)-OCT (top right) images from the same eye. The external limiting membrane (ELM) was marked on each OCT B-scan (middle left) + (middle right) where clearly visible using the Pencil tool from Adobe Photoshop. ELM was visible across 77% of the FDOCT scan (bottom left) in contrast to 59% of the TDOCT scan (bottom right) from the same eye.

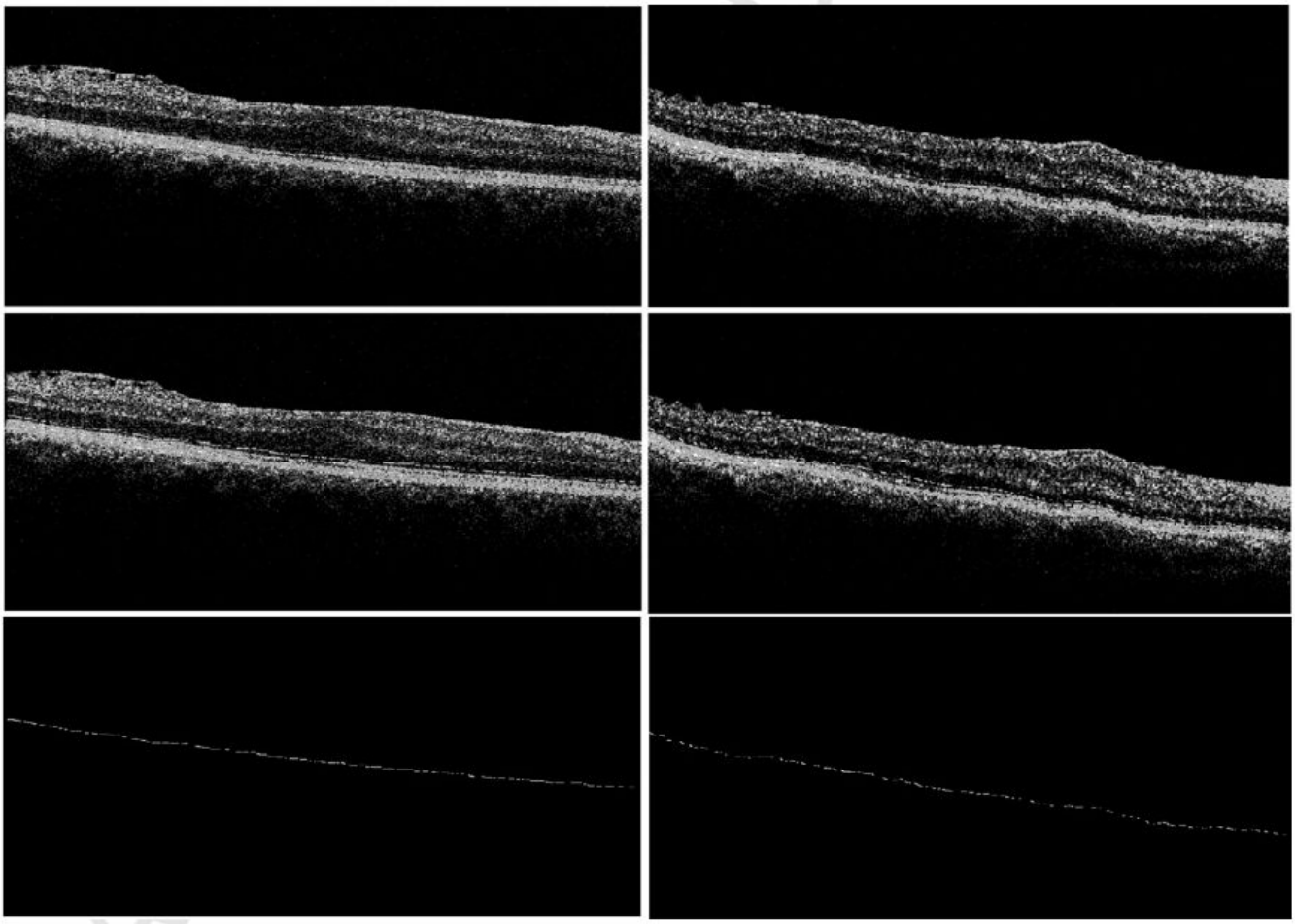

**Figure 3.**
Time domain (TD)-OCT (first row) and Fourier domain (FD)-OCT (second row) B-scans showing subfoveal photoreceptor outer segment disruption (white box). TDOCT (third row) and FDOCT (fourth row) B-scans showing more widespread disruption (white box).

## Table 1

**Comparison of time domain and Fourier domain optical coherence tomography: Preretinal space and Macular Holes**

| Clinical Finding | Time domain OCT Sensitivity % (95% CI) | Fourier domain OCT Sensitivity % (95% CI) | Time domain OCT Sensitivity without Questionables % (95% CI) | Fourier domain OCT Sensitivity without Questionables % (95% CI) |
|---|---|---|---|---|
| **Preretinal Space** | | | | |
| Hyaloid Face | 73.3 (44.9 – 92.2) | 100 (78.2 – 100) | 46.7 (21.3 – 73.4) | 100 (78.2 – 100) |
| Vitreomacular Traction | 42.9 (9.9 – 81.6) | 100 (59 – 100) | 100 (2.5 – 100) | 100 (2.5 – 100) |
| Epiretinal Membrane | 63.6 (40.7 – 82.8) | 95.5 (77.2 – 99.9) | 75 (47.6 – 92.7) | 100 (79.4 – 100) |
| **Macular Holes** | | | | |
| Lamellar Hole | 40 (5.27 – 85.3) | 60 (14.7 – 94.7) | 50 (1.26 – 98.7) | 50 (1.26 – 98.7) |
| Full-Thickness Macular Hole | 100 (2.5 – 100) | 100 (2.5 – 100) | 100 (2.5 – 100) | 100 (2.5 – 100) |

## Table 2

**Comparison of time domain and Fourier domain optical coherence tomography: Retina, Subretinal Space, and Retinal Pigment Epithelium**

| Clinical Finding | Time Domain OCT Sensitivity % (95% CI) | Fourier domain OCT Sensitivity % (95% CI) | Time domain OCT Sensitivity without Questionables % (95% CI) | Fourier domain OCT Sensitivity without Questionables % (95% CI) |
|---|---|---|---|---|
| **Retinal Findings** | | | | |
| Intraretinal Cystoid Space | 86.2 (68.3 – 96.1) | 82.8 (64.2 – 94.2) | 76 (54.9 – 90.6) | 84 (63.9 – 95.5) |
| Diffuse Intraretinal Edema | 60.9 (38.5 – 80.3) | 87 (66.4 – 97.2) | 42.1 (20.3 – 66.5) | 100 (82.4 – 100) |
| Highly Reflective Intraretinal Interface | 48.4 (30.2 – 66.9) | 90.3 (74.2 – 98) | 50 (28.2 – 71.8) | 90.9 (70.8 – 98.9) |
| External Limiting Membrane | 62.8 (46.7 – 77) | 100 (91.8 – 100) | 45 (29.3 – 61.5) | 100 (91.2 – 100) |
| Photoreceptor Outer Segment Disruption | 33.3 (13.3 – 59) | 94.4 (72.7 – 99.9) | 20 (4.33 – 48.1) | 93.3 (68.1 – 99.8) |
| **Subretinal Findings** | | | | |
| Subretinal Fluid | 46.2 (19.2 – 74.9) | 100 (75.3 – 100) | 66.7 (29.9 – 92.5) | 100 (66.4 – 100) |
| Subretinal Tissue | 61.5 (31.6 – 86.1) | 100 (75.3 – 100) | 50 (18.7 – 81.3) | 60 (26.2 – 87.8) |
| **Retinal Pigment Epithelium** | | | | |
| Large PED | 81 (58.1 – 94.6) | 100 (83.9 – 100) | 77.8 (52.4 – 93.6) | 100 (81.5 – 100) |
| Triple Highly Reflective Band at Level of RPE* | 17.6 (3.8 – 43.4) | 100 (80.5 – 100) | 16.7 (2.09 – 48.4) | 100 (73.5 – 100) |
| Small PED/Drusen | 82.1 (63.1 – 93.9) | 92.9 (76.5 – 99.1) | 66.7 (46 – 83.5) | 100 (87.2 – 100) |
| Bruch Membrane | 58.8 (32.9 – 81.6) | 100 (80.5 – 100) | 66.7 (34.9 – 90.1) | 100 (73.5 – 100) |

* "Triple Highly Reflective Band at Level of RPE" refers to the three outer retinal bands believed to correspond (from inner to outer) to: (1) the photoreceptor inner segment-outer segment junction, (2) interface between photoreceptors and RPE (the inner RPE surface), and (3) the outer RPE surface. In lower quality scans, the latter two bands may be merged into a single band.